

Precision cosmology from X-ray AGN clustering

Spyros Basilakos¹ and Manolis Plionis^{2,3}

¹Academy of Athens, Research Center for Astronomy & Applied Mathematics, Soranou Efessiou 4, 11-527 Athens, Greece

²Institute of Astronomy & Astrophysics, National Observatory of Athens, I. Metaxa & V. Pavlou, Palaia Penteli, 15236 Athens, Greece

³Instituto Nacional de Astrofísica, Óptica y Electrónica (INAOE) Apartado Postal 51 y 216, 72000 Puebla, Pue., Mexico

Accepted 2009 September 13. Received 2009 August 24; in original form 2009 July 8

ABSTRACT

We place tight constraints on the main cosmological parameters of spatially flat cosmological models by using the recent angular clustering results of *XMM–Newton* soft (0.5–2 keV) X-ray sources, which have a redshift distribution with a median of $z \sim 1$. Performing a standard likelihood procedure, assuming a constant in comoving coordinates active galactic nuclei (AGN) clustering evolution, the AGN bias evolution model of Basilakos, Plionis & Ragone-Figueroa and the *Wilkinson Microwave Anisotropy Probe* value of σ_8 , we find stringent simultaneous constraints in the (Ω_m, w) plane, with $\Omega_m = 0.26 \pm 0.05$, $w = -0.93^{+0.11}_{-0.19}$.

Key words: cosmological parameters.

1 INTRODUCTION

Recent studies in observational cosmology, using all the available high-quality cosmological data [Type Ia supernovae (SNIa), cosmic microwave background (CMB), baryonic acoustic oscillations (BAO), etc.], converge to an emerging ‘standard model’, which is flat, and it is described by the Friedmann equation: $H^2(a) = 8\pi G[\rho_m(a) + \rho_Q(a)]/3$, with $a(t)$ the scalefactor of the universe, $\rho_m(a)$ the density corresponding to the sum of baryonic and cold dark matter (CDM) and an extra component $\rho_Q(a)$ with negative pressure called dark energy and needed to explain the observed accelerated cosmic expansion (e.g. Davis et al. 2007; Kowalski et al. 2008; Hicken et al. 2009; Komatsu et al. 2009 and references therein).

The nature of the dark energy is currently one of the most fundamental and difficult puzzles in physics and cosmology. Indeed, during the last decade there has been an intense theoretical debate among cosmologists regarding the nature of the exotic ‘dark energy’. Due to the absence of a physically well-motivated fundamental theory, various candidates have been proposed in the literature, among which are a cosmological constant (constant vacuum), a time varying vacuum quintessence, k -essence, vector fields, phantom, tachyons, Chaplygin gas, and the list goes on (e.g. Ozer & Taha 1987, Weinberg 1989; Wetterich 1995; Caldwell, Dave & Steinhardt 1998; Brax & Martin 1999; Peebles & Ratra 2003; Brookfield et al. 2006; Boehmer & Harko 2007 and references therein). The simplest type of dark energy corresponds to a scalar field having a self-interaction potential $V(\phi)$, with the field energy density decreasing with a slower rate than the matter energy density (dubbed also ‘quintessence’; e.g. Peebles & Ratra 2003 and references therein), and the dark energy component being described by an equation of state $p_Q = w\rho_Q$ with $w < -1/3$. Note that a redshift dependence of the equation of state parameter is also possible, but its present

functional form is phenomenologically based (see Chevallier & Polarski 2001; Linder 2003). A particular case of ‘dark energy’ is the traditional cosmological constant (Λ) model (corresponding to $w = -1$), which appears to be supported by the combined analysis of the recent relevant observational data (e.g. Komatsu et al. 2009 and references therein).

It has been shown that the application of the correlation function analysis on samples of high-redshift galaxies or X-ray-selected active galactic nuclei (AGN) can be used as a useful tool for cosmological studies (e.g. Matsubara 2004, Basilakos & Plionis 2005; 2006). The scope of the present study is along the same lines, i.e. to place constraints on the (Ω_m, w) parameter space of spatially flat cosmological models using a single cosmologically relevant experiment, i.e. that of the recently derived clustering properties of the *XMM–Newton* soft (0.5–2 keV) X-ray point sources (Ebrero et al. 2009a).

2 OBSERVED AND PREDICTED CORRELATIONS

2.1 X-ray AGN correlations

Recently, Ebrero et al. (2009a) derived the angular correlation function of the soft (0.5–2 keV) X-ray sources using 1063 *XMM–Newton* observations at high galactic latitudes (hereafter *2XMM*). A full description of the data reduction, source detection and flux estimation is presented in Mateos et al. (2008). In brief, the survey contains $\sim 30\,000$ point sources within an effective area of ~ 125.5 deg² (for an effective flux limit of $f_x \geq 1.4 \times 10^{-15}$ erg cm⁻² s⁻¹). Also, Ebrero et al. (2009a) present the details regarding the angular correlation function estimation, the various biases that should be taken into account (the amplification bias and integral constraint), the survey luminosity and selection functions as well as issues related to possible non-AGN contamination, which are estimated to be $\lesssim 10$ per cent.

*E-mail: svasil@academyofathens.gr

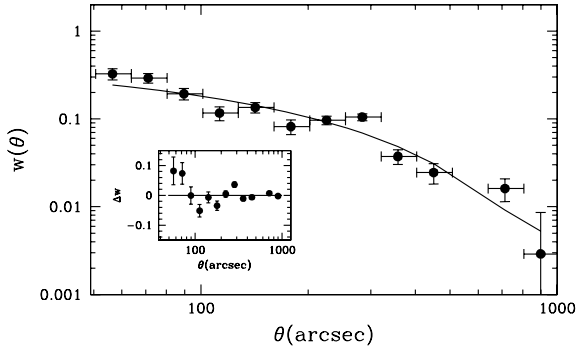


Figure 1. The two-point angular correlation function of the soft band (Ebrero et al. 2009a). The solid line represents the theoretical angular correlation function for the best-fitting ($\Omega_m = 0.26$ and $w = -0.93$) cosmological model. Inset: the residual angular correlation function between observations and theory with 2σ uncertainties.

The redshift selection function of the X-ray sources, derived by using the soft-band luminosity function of Ebrero et al. (2009b) which takes into account the realistic luminosity-dependent density evolution of the X-ray sources, predicts a characteristic depth of $z \sim 1$.

In Fig. 1, we present the X-ray AGN angular correlation function of the Ebrero et al. (2009a) analysis. The solid points correspond to the observed angular correlation function while the solid line represents the theoretical angular correlation function for the best-fitting cosmological model (see further below). The inset panel of Fig. 1 shows the residual, $\Delta w(\theta)$, between observations and theory. There appears to be an interesting sinusoidal variation with θ , which merits further investigation. Unaccounted non-linear effects, at the smallest angular separations, could be the cause of the large Δw values at $\theta < 80$ arcsec.

2.2 From angular to spatial clustering

We briefly present the main points of the method used to put cosmological constraints using the angular clustering of some extragalactic mass tracer. A first important ingredient is the use of Limber's formula which relates the angular, $w(\theta)$, and the spatial, $\xi(r)$, correlation functions. Assuming flatness, the Limber's equation can be written as

$$w(\theta) = 2 \frac{\int_0^\infty \int_0^\infty x^4 \phi^2(x) \xi(r, z) dx du}{\left[\int_0^\infty x^2 \phi(x) dx \right]^2}, \quad (1)$$

where $\phi(x)$ is the AGN redshift selection function (the probability that a source at a distance x is detected in the survey), and x is the coordinate distance related to the redshift through $x(z) = c \int_0^z \frac{dy}{H(y)}$ with $H(z) = H_0 [\Omega_m(1+z)^3 + \Omega_Q(1+z)^{3(1+w)}]^{1/2}$ and $\Omega_Q = 1 - \Omega_m$. Also, r is the physical separation between two sources having an angular separation, θ , which in the small angle approximation is given by $r \simeq (1+z)^{-1}(u^2 + x^2\theta^2)^{1/2}$ (with u being the line-of-sight separation of any two sources). The number of AGN within a shell ($z, z + dz$) is given by

$$\frac{dN}{dz} = \delta\omega_s x^2(z) n_s \phi(x) \left(\frac{c}{H_0} \right) E^{-1}(z), \quad (2)$$

where $\delta\omega_s (\simeq 125.5 \text{ deg}^2)$ is the effective solid angle of the survey, $E(z) = H(z)/H_0$ and n_s is the comoving AGN number density at $z = 0$. The source redshift distribution dN/dz , as already mentioned previously, is estimated by integrating the appropriate (Ebrero et al. 2009b) luminosity function, folding in the area curve of the survey.

Inserting equation (2) into equation (1), we have after some algebra that

$$w(\theta) = 2 \frac{H_0}{c} \int_0^\infty \left(\frac{1}{N} \frac{dN}{dz} \right)^2 E(z) dz \int_0^\infty \xi(r, z) du. \quad (3)$$

The spatial correlation function can be written as $\xi(r, z) = (1+z)^{-(3+\epsilon)} b^2(z) \xi_{DM}(r)$, with $\xi_{DM}(r)$ indicating the predicted spatial correlation function of the underlying matter distribution (see below) and ϵ parametrizing the type of AGN clustering evolution (e.g. de Zotti et al. 1990), and following Kúndic (1997) and Basilakos & Plionis (2005, 2006) we use here the constant in comoving coordinates clustering model, i.e. $\epsilon = -1.2$. Also, $b(z)$ is the evolution of the linear bias factor which is an essential ingredient for CDM models in order to reproduce the observed mass-tracer distribution (cf. Kaiser 1984; Davis et al. 1985; Bardeen et al. 1986; Benson et al. 2000). In the current analysis, we use our bias evolution model (Basilakos, Plionis & Ragono-Figueroa 2008), which is based on the solution of a second-order differential equation derived by using linear perturbation theory and the Friedmann–Lemaître solutions of the cosmological field equations. Our model was initially presented in Basilakos & Plionis (2001, 2003) and has been recently extended to include the effects of halo interactions and merging (for details see Basilakos et al. 2008).

2.3 Theoretically predicted clustering

We estimate the theoretically predicted spatial correlation function of the underlying matter distribution, $\xi_{DM}(r)$, from the Fourier transform of the spatial power spectrum $P(k)$:

$$\xi_{DM}(r) = \frac{1}{2\pi^2} \int_0^\infty k^2 P(k) \frac{\sin(kr)}{kr} dk, \quad (4)$$

where $P(k)$ denotes the power of the matter fluctuations linearly extrapolated to the present epoch. We consider the CDM power spectrum, $P(k) = P_0 k^n T^2(k)$, with $T(k)$ being the CDM transfer function and $n \simeq 0.96$ following the 5-year *WMAP* results (Komatsu et al. 2009). In order to define the functional form of the power spectrum, we utilize the transfer function parameterization as in Bardeen et al. (1986), with the approximate corrections given by Sugiyama (1995). The rms fluctuations of the linear density field on mass scale M is

$$\sigma(M) = \left[\frac{1}{2\pi^2} \int_0^\infty k^2 P(k) W^2(kR) dk \right]^{1/2}, \quad (5)$$

where the window function is given by $W(kR) = 3(\sin kR - kR \cos kR)/(kR)^3$ and $R = (3M/4\pi\rho_0)^{1/3}$. The parameter ρ_0 denotes the mean matter density of the universe at the present time ($\rho_0 = 2.78 \times 10^{11} \Omega_m h^2 \text{ M}_\odot \text{ Mpc}^{-3}$). The normalization of the power spectrum is given by $P_0 = 2\pi^2 \sigma_8^2 \left[\int_0^\infty T^2(k) k^{n+2} W^2(kR_8) dk \right]^{-1}$ where σ_8 is the rms mass fluctuation on $R_8 = 8 h^{-1} \text{ Mpc}$ scales and for which we use the *WMAP5* value of $\sigma_8 \simeq 0.8$ (Komatsu et al. 2009). It is worth noting that we also use the non-linear corrections introduced by Peacock & Dodds (1994).

2.4 Cosmological constraints

In order to constrain the cosmological parameters we use, as in Basilakos & Plionis (2005), a standard χ^2 likelihood procedure and compare the measured *XMM* soft source angular correlation function (Ebrero et al. 2009a) with the predictions of different spatially flat cosmological models. To this end we use the likelihood

estimator,¹ defined as $\mathcal{L}_{\text{AGN}}(\mathbf{p}) \propto \exp[-\chi_{\text{AGN}}^2(\mathbf{p})/2]$ with

$$\chi_{\text{AGN}}^2(\mathbf{p}) = \sum_{i=1}^n \frac{[w_{\text{th}}(\theta_i, \mathbf{p}) - w_{\text{obs}}(\theta_i)]^2}{\sigma_i^2 + \sigma_{\theta_i}^2}, \quad (6)$$

where \mathbf{p} is a vector containing the cosmological parameters that we want to estimate, σ_i is the uncertainty of the observed angular correlation function and σ_{θ_i} corresponds to the width of the angular separation bins.

As we have previously mentioned, we work within the framework of a flat cosmology with primordial adiabatic fluctuations and baryonic density of $\Omega_b h^2 = 0.022 (\pm 0.002)$ (e.g. Komatsu et al. 2009), while utilizing the *Hubble Space Telescope* key project results of Freedman et al. (2001) we fix the Hubble constant to $H_0 \simeq 71 \text{ km s}^{-1} \text{ Mpc}^{-1}$ (see also Komatsu et al. 2009). Note that since we fix, in the following analysis, the values of both H_0 and Ω_b , we do not take into account their quite small uncertainties.

The corresponding statistical vector that we have to fit is $\mathbf{p} \equiv (\Omega_m, w, M_h)$, where M_h is the host dark matter halo mass, which enters in our biasing evolution scheme (see Basilakos, Plionis & Ragone-Figueroa 2008). Note also that the normalization of the power spectrum, σ_8 , could have been left as a free parameter (see Basilakos & Plionis 2006), but in this work we choose to use the well-established *WMAP5* value (see the previous section). We sample the various parameters as follows: the matter density $\Omega_m \in [0.01, 1]$ in steps of 0.01; the equation of state parameter $w \in [-1.6, -0.34]$ in steps of 0.01 and the parent dark matter halo $M_h/10^{13} h^{-1} M_{\odot} \in [0.1, 4]$ in steps of 0.01.

We find that the likelihood function of the soft X-ray sources peaks at $\Omega_m = 0.26 \pm 0.05$, $w = -0.93_{-0.19}^{+0.11}$ and $M_h = 2_{-0.2}^{+0.3} \times 10^{13} h^{-1} M_{\odot}$, with a reduced χ^2 of ~ 4 . Such a large value is caused by the small $w(\theta)$ uncertainties in combination with the observed modulation (see inset panel of Fig. 1). Had we used a $2\sigma w(\theta)$ uncertainty in equation (6), we would have obtained roughly the same constraints and a reduced χ^2 of ~ 1 (see the upper-right panel of Fig. 2).

In the upper-left panel of Fig. 2, we present the current constraints in the (Ω_m, w) plane by marginalizing our solution over M_h (thick solid lines). For comparison reasons, we also show our previous solutions of Basilakos & Plionis (2005, 2006), which were based on the shallow *XMM/2dF* survey ($\sim 2.3 \text{ deg}^2$) which contains only 432 point sources (with an effective flux limit of $f_x \geq 2.7 \times 10^{-14} \text{ erg cm}^{-2} \text{ s}^{-1}$). In particular, the dotted lines correspond to a solution using $\sigma_8 \simeq 0.93$ (Basilakos & Plionis 2005), while the dashed lines to the corresponding solution for $\sigma_8 \simeq 0.74$ (Basilakos & Plionis 2006). Comparing our present analysis with our previous results, it becomes evident that with the current high-precision X-ray AGN correlation function of Ebrero et al. (2009a) we have achieved to place simultaneously quite stringent constraints on both, w and Ω_m .

Regarding other analyses of cosmological data, it is interesting to note that Davis et al. (2007) using the combined analysis of the SNIa+BAO+CMB found $\Omega_m = 0.27 \pm 0.04$ and $w = -1.01 \pm 0.15$, while a similar analysis of Kowalski et al. (2008), using a newer SNIa compilation, provided $\Omega_m = 0.274 \pm 0.016$ with $w = -0.969 \pm 0.06$ (see also corresponding results in Komatsu et al. 2009 and Hicken et al. 2009). We would like to stress that despite the fact that we use a single cosmologically relevant experiment, i.e. *the observed angular correlation function of the soft X-ray sources*, our results coincide within 1σ with the results of the joint analysis,

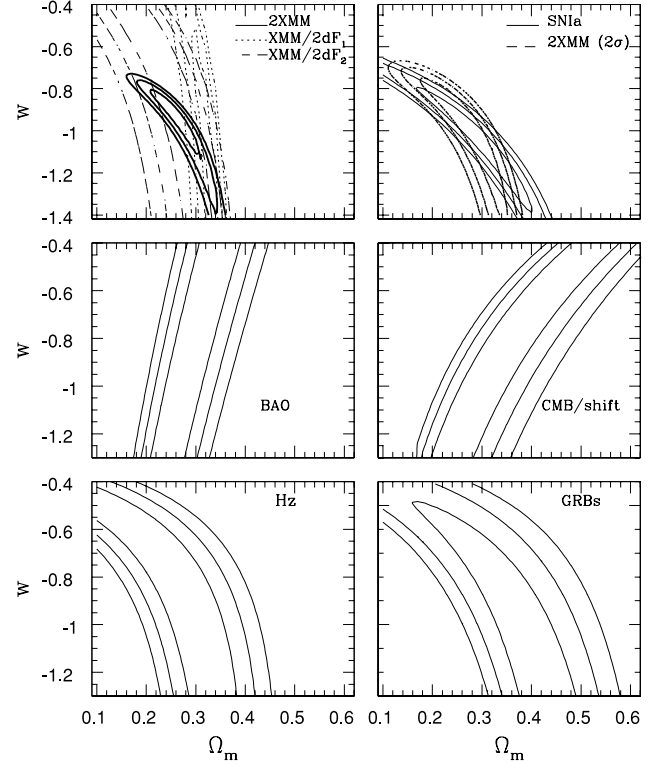


Figure 2. Likelihood contours (1σ , 2σ and 3σ) in the (Ω_m, w) plane. The upper-left panel shows the results based on the current (solid lines) and previous *XMM* source clustering analyses. In the upper right panel, we show the results based on the SNIa (solid lines) and the *XMM* clustering results and a 2σ clustering uncertainty (dashed lines). The rest of the panels correspond to the cosmological data indicated. The contours are plotted where $-2\ln\mathcal{L}/\mathcal{L}_{\text{max}}$ is equal to 2.30, 6.16 and 11.83.

discussed previously. Therefore, the X-ray-selected AGN appear to be ideal tools for extracting cosmological information. In order to further illustrate such a claim, we perform further below a direct comparison between our results with those derived by other *single* cosmological data sets.

2.5 Comparison with other cosmological data

We present here a comparison between the (Ω_m, w) solution space provided by our analysis of the *XMM-Newton* X-ray sources with those derived using other cosmological data. The goal is to give the reader the opportunity to appreciate the relative strength and precision of the different methods. Therefore, we present in Fig. 2 the 1σ , 2σ and 3σ confidence levels in the (Ω_m, w) plane, provided by the different cosmological data presently available. These are (a) the Hubble relation based on the latest sample of 397 supernovae of Hicken et al. (2009), (b) the dimensionless distance to the surface of the last scattering $R = 1.71 \pm 0.019$ (Komatsu et al. 2009), (c) the baryon acoustic oscillation distance at $z = 0.35$, $A = 0.469 \pm 0.017$ (Eisenstein et al. 2005; Padmanabhan et al. 2007), (d) the Hubble function (H_z) derived directly from nine early-type galaxies at high redshifts (Simon, Verde & Jimenez 2005) and (e) the Hubble relation based on a sample of 69 gamma-ray bursts (Cardone, Capozziello & Dainotti 2009). It is evident that the X-ray AGN clustering likelihood analysis alone puts the most stringent constraints on the value of the equation of state parameter. To be fair, however, we must stress that in our analysis we have a priori

¹ Likelihoods are normalized to their maximum values.

imposed the value of σ_8 to that of the *WMAP5* (Komatsu et al. 2009), which does not enter the other cosmological tests. However, the size of the solution space, for any plausible value of σ_8 , is as small as for the nominal case used, the only difference would be a tilt of the contours, as can be appreciated by the two *XMM/2dF* solution spaces in the upper-left panel of Fig. 2.

Note that if we increase the uncertainty of the observed X-ray source angular correlation function by a factor of 2, then the resulting contours (thick dashed lines in the right-hand panel of Fig. 2) closely match those of the most recent SNIa analysis. In a forthcoming paper (Plionis et al. in preparation), we will present details of a joint analysis of our X-ray-selected AGN results with that of all other cosmologically relevant data.

Finally, we have to caution the reader of two (reasonable, we believe) assumptions that enter a priori in our analysis: (1) that the clustering evolution of X-ray-selected AGN is constant in comoving coordinates (the effects of other evolution models have been investigated in Basilakos & Plionis 2005) and (2) that the Basilakos et al. (2008) bias evolution model is the appropriate one, which is supported by a comparison with N -body simulations and available clustering data (see figs 1 and 3 of Basilakos et al. 2008).

3 CONCLUSIONS

We have utilized the recent determination of the clustering properties of high- z X-ray-selected AGN, identified as soft (0.5–2 keV) point sources (Ebrero et al. 2009a), in order to constrain the main cosmological parameters. We find that the X-ray AGN clustering likelihood analysis alone, within the context of flat cosmological models, can place tight constraints on the main cosmological parameters (Ω_m , w), and indeed relatively tighter than any other single observational method to date. The current analysis provides a best spatially flat model with $\Omega_m = 0.26 \pm 0.05$ and $w = -0.93^{+0.11}_{-0.19}$.

ACKNOWLEDGMENTS

We are greatly thankful to Dr J. Ebrero for comments and for providing us with an electronic version of their clustering results and their *XMM* survey area curve. MP also acknowledges financial support under Mexican government CONACyT grant 2005-49878.

REFERENCES

- Bardeen J. M., Bond J. R., Kaiser N., Szalay A. S., 1986, *ApJ*, 304, 15
 Basilakos S., Plionis M., 2001, *ApJ*, 550, 522
 Basilakos S., Plionis M., 2003, *ApJ*, 593, L61
 Basilakos S., Plionis M., 2005, *MNRAS*, 360, L35
 Basilakos S., Plionis M., 2006, *ApJ*, 650, L1
 Basilakos S., Plionis M., Ragone-Figueroa C., 2008, *ApJ*, 678, 627
 Benson A. J., Cole S., Frenk S. C., Baugh M. C., Lacey G. C., 2000, *MNRAS*, 311, 793
 Boehmer C. G., Harko T., 2007, *Eur. Phys. J.*, C50, 423
 Brax P., Martin J., 1999, *Phys. Lett.*, B468, 40
 Brookfield A. W., van de Bruck C., Motta D. F., Tocchini-Valentini D., 2006, *Phys. Rev. Lett.*, 96, 061301
 Caldwell R. R., Dave R., Steinhardt P. J., 1998, *Phys. Rev. Lett.*, 80, 1582
 Cardone V. F., Capozziello S., Dainotti M. G., 2009, *MNRAS*, in press (arXiv:0901.3194)
 Chevallier M., Polarski D., 2001, *Int. J. Mod. Phys. D*, 10, 213
 Davis M., Efstathiou G., Frenk C. S., White S. D. M., 1985, *ApJ*, 292, 371
 Davis T. M. et al., 2007, *ApJ*, 666, 716
 de Zotti G., Persic M., Franceschini A., Danese L., Palumbo G. G. C., Boldt E. A., Marshall F. E., 1990, *ApJ*, 351, 22
 Ebrero J., Mateos S., Stewart G. C., Carrera F. J., Watson M. G., 2009a, *A&A*, 500, 749
 Ebrero J. et al., 2009b, *A&A*, 493, 55
 Eisenstein D. J. et al., 2005, *ApJ*, 633, 560
 Freedman W. L. et al., 2001, *ApJ*, 553, 47
 Hicken M. et al., 2009, *ApJ*, 700, 1097
 Kaiser N., 1984, *ApJ*, 284, L9
 Komatsu E. et al., 2009, *ApJS*, 180, 330
 Kowalski M. et al., 2008, *ApJ*, 686, 749
 Kúndic T., 1997, *ApJ*, 482, 631
 Linder E. V., 2003, *Phys. Rev. Lett.*, 90, 091301
 Mateos S. et al., 2008, *A&A*, 429, 51
 Matsubara T., 2004, *ApJ*, 615, 573
 Ozer M., Taha O., 1987, *Nucl. Phys.*, B287, 776
 Padmanabhan N. et al., 2007, *MNRAS*, 378, 852
 Peebles P. J. E., Ratra B., 2003, *Rev. Mod. Phys.*, 75, 559
 Peacock A. J., Dodds S. J., 1994, *MNRAS*, 267, 1020
 Simon J., Verde L., Jimenez R., 2005, *Phys. Rev. D.*, 71, 123001
 Sugiyama N., 1995, *ApJS*, 100, 281
 Weinberg S., 1989, *Rev. Mod. Phys.*, 61, 1
 Wetterich C., 1995, *A&A*, 301, 321

This paper has been typeset from a $\text{\TeX}/\text{\LaTeX}$ file prepared by the author.